IJCSME
OPEN ACCESS

Special Issue on Computational Science, Mathematics and Biology
IJCSME- SCSMB-16-March-2016
ISSN-2349-8439

Ligand based 3D-QSAR approach of EGFR

[1]Sandeep Swargam, [1a]Hema Kanipakam, [1b]Pradeep Natarajan, , [2]M.M. Suchitra, [3]Rajeswari Jinka and [1c]Amineni Umamaheswari

Abstract: This Human epidermal growth factor receptor (EGFR) family is one of the most studied protein family in various cell signaling mechanisms. It contains four membrane bound receptors namely epidermal growth factor receptor 1-4.Aberrant activation of ErbB receptor family proteins and their role in intra cellular signaling mechanisms and their mutations lead to cause the numerous human diseases. The first generation inhibitors failed to bind with the EGFR due to T790M mutation. The second generation inhibitors overcome the resistance when compared to the first generation compounds but failed in approval level. Reported publication data given a clear idea to develop new class inhibitors against the EGFR proteins. In this study, ligand based pharmacophore modeling and 3D-QSAR studies were carried out with the 100 ligands of EGFR. Fifteen pharmacophore hypotheses were developed and common AADRR hypothesis was selected for QSAR analysis. Further the model was screened against the 3D database of twenty million entries and 1436 structure analogues were obtained and subjected to XP docking with EGFR grid in GLIDE. One lead molecule is having the best binding interactions than the existing inhibitors. Lead 1 is further subjected to QPLD, IFD, binding free energy and molecular dynamics studies which deciphered better binding interactions with EGFR. Thus lead1was proposed as a novel lead against the EGFR.

Keywords:EGFR, Cancer, Ligand based pharmacophore modeling, QSAR and molecular docking analysis.

Introduction

Human epidermal growth factor receptor (EGFR) family is one of the most studied protein kinase family in various cell signal transduction mechanisms and regulate the cellular functions [1,2]. It contains four membrane bound receptors namely epidermal growth factor receptor-1(EGFR, Her1, erbB1), EGFR2/Her2/erbB2/neu, EGFR3/ Her3/erbB3 and EGFR4/Her4/erbB4 [3,4]. These four are structurally related and shares similar molecular scaffolds in the structural moiety [3,4]. Each of the protein comprises of extra cellular ligand binding site (I-IV), hydrophobic transmembrane region and cytoplasmic binding region. In case of cytoplasmic region, contains the conserved catalytic domain and auto phosphorylation site regions present on the carboxy terminal [3-6]. Activation of EGFR signaling is through the ligand induced stabilization of homo/hetero demonization which is sequentially followed by auto phosphorylation mechanisms. This process activates the downstream stimuli of Ras/Raf/MAPK and PI3K/Akt/mTOR pathways.

[1]DEPARTMENT OF BIOINFORMATICS,
[2]DEPARTMENT OF BIOCHEMISTRY
[3]DEPARTMENT OF BIOCHEMSOTRY,
ACHARYA NAGARAJUNA UNIVERSITY
SVIMS UNIVERSITY,GUNTUR,
INDIATIRUPATI, INDIA.
Email: svims.btisnet@nic.in

Aberrant activation of EGFR receptor family proteins and their role inintra cellular signaling mechanisms and their mutations leads to cause the numerous human namely cancers, diabetes, inflammation, bone disorders, arteriosclerosis and angiogenesis [5-7]. Among the four proteins, EGFR1 is the attractive target which is directly linked with human tumors. In cancers, over expression of the EGFR is associated with the human epithelial cancers namely lung, anal and glioblastoma and in solid human cancers namely non-small cell lung cancer, breast, bladder, ovarian, colorectal, pancreatic, ovarian and head and neck cancers [5-10]. The role of EGFR in various cancers, sheds the important platform to design novel anti cancer agents to inhibit the over expression levels of EGFR [7-10]. Different types such as specific, reversible, irreversible and dual inhibitors are available for human EGFR. The first generation reversible inhibitors like Erlotinib, gefitinib and laptinib initially prevent the autophosphorylation of the EGFR [11-15] but due to T790M mutation these inhibitors failed to bind with EGFR [16-20].The second generation inhibitors like HKI-272, EKB-569, BIBW2992 and PF00299804 were developed to overcome the resistance to the first generation compounds [21]. These irreversible compounds showed promising results during the clinical level studies and but failed in approval level [22-23]. Afatinib was approved in 2013 for non-small cell lung cancer and clinical investigations are still ongoing to other cancer [24]. In this study, with reported 100 EGFR inhibitors we performed ligand based pharmacophore modeling,3D-QSAR model generation, geometrical shape based screening and multiple docking methodologies to explore the development of novel leads against the protein.

Materials and Methods

3D-QSAR analysis, molecular docking and dynamics were carried out in Centos 5.0 LINUX platform installed in HPZ 800 work station using Schrodinger LLC, New York, 2014.

1. Dataset

First, 100 molecules having biological inhibition activity (IC50) ~ 4 to 9 nM against EGFR were collected [25] and pIC50 of the compounds were predicted [26].The dataset was divided into 35 actives, 25 moderates and40 inactive

compounds based on inhibition activity. PHASE module was used to convert the 2D structures into 3D structures and cleaning and minimization of structures were carried out with LigPrep [27] module in OPLS-2005 force filed [28]. Conformers were generated for each minimized ligand using rapid torsion angle search and minimization was carried out using the MMFF (Merck Molecular Force Field), with an implicit GB/SA (Generalized-Born/Surface Area) solvent model [24].

2. Common pharmacophore hypothesis (CPH)

PHASE supplies a built of six-pharmacophore sites which includes hydrogen bond acceptor (A), hydrogen bond donor (D), hydrophobic group (H), aromatic ring (R), negatively charged group (N) and positively charged group (P) [29]. Active analog approach was applied to identify the common pharmacophore hypothesis. Ligand conformers were culled from the set of active ligand using tree based partitioning technique according to their inter site distances between the each pair of sites in the obtained pharmacophore [30]. Scoring function was carried out to the best aligned defined active set of ligands.

3. QSAR building and validation

Based on low to higher inhibition values the dataset was divided into 65compounds as trainee set and 35 as test set by incorporating biological and chemical diversity to generate atom-based QSAR models. For each model, three or five partial least squares (PLS) factors were generated which tend to fit pIC values beyond their experimental uncertainty [31-32]. The generated model was validated using the external test set compounds which are not considered during the model generation.

4. Shape based screening

The validated QSAR model was used for shape based screening against in-house library of 20 million compounds in PHASE and obtained 1436 conformers. All conformers were further filtered by Lipinski's filters.

5. Protein preparation, molecular docking and free energy calculations

Human EGFR (4I22) [33] was prepared by adding hydrogen atoms and removal of unwanted water molecules from the protein structure in protein preparation wizard. In GLIDE, 10 ÅX 10Å X 10 Å grid box was defined around the ligand binding site on 4I22. A systematic three tier rigid receptor docking (RRD) docking protocol, which include high throughput virtual screening (HTVS), standard precision (SP), extra precision (XP) docking methods were implemented. The best ranked compounds from the GLIDEXP docking were applied for MM-GBSA analysis [29, 34]. The binding energy is calculated by the following equation:

$\Delta Gbind = \Delta E + \Delta Gsolv + \Delta GSA$

Further the best hits were subjected to Quantum polarized ligand docking (QPLD), MM-GBSA analysis and further the best lead1-EGFRcomplex was implemented to induced fit docking (IFD) and MM-GBSA analysis [29,30].

6. Molecular dynamics (MD) simulations

MD simulations for 4I22- lead1 docking complex were performed to evaluate the stability and conformational changes during 50ns simulations using Desmond v3.5. Energy and inter molecular interactions of the docking complex in each trajectory were examined.

7. ADMET predictions

The best lead was further analyzed for ADME/T (adsorption, distribution, metabolism, excretion and toxicity) properties to know drug-likeliness using QikProp.

Results and Discussion

1. Dataset

The dataset of 100 compounds were divided in to 30 active compounds (< 8.0 μM) 30 were moderate active compounds and 40 inactive set (> 7.0μM).

2. Common pharmacophore hypothesis (CPH) analysis

Fifteen possible pharmacophore variants were developed with diverse set of active molecules with maximum (5) and minimum (3) number of pharmacophore sites. CPH analysis yielded one hypothesis from 15 models in three different phases of PHASE scoring procedure which includes survival score, survival inactive score and post-hoc score. Therefore, the best hypothesis (AADRR) was used for the generation of QSAR model.

3. QSAR model analysis

In general for performing the QSAR study, trainee set and test set should be in a 4:1 ratio [35]. So, dataset was divided into 65 training set and 35 test set compounds and aligned to inactive or moderately active molecules based on matching criteria with at least three pharmacophore features.

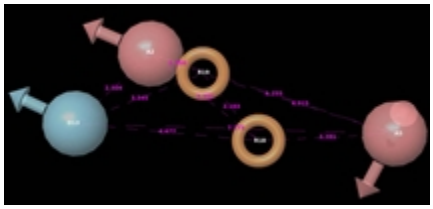

Fig.1: QSAR model with pharmacophore features AADRR orange torus indicate aromatic ring, pink sphere indicates acceptor feature, light blue sphere indicate donor feature

R2 value of the best QSAR model should have >0.6 [36] and AADRR.10 model showed R2 of 0.85.Validation of the model was further carried with the regression analysis of 65 trainee set molecules which gave an excellent correlation coefficient (R) value of 0.84 revealing the good predictive

DOI: 10.18645/IJCSME.SPB.0004

capacity of AADRR.10 model (Fig. 2(A)) . Experimental predicated activity of the external dataset of 35 test set molecules were cross checked with the diverse activities which gave an excellent correlation coefficient (R) value of 0.85 (Fig. 2(B))revealing the good predictive capacity of the AADRR.10 model. PLS regression was used to generate 3D cubic analysis of model which impulse the different properties of obtained molecule such as hydrogen bond acceptor, hydrogen bond donor, hydrophobic group, positive and negative ionic features. Generated QSAR model was validated using the external dataset of 35 test set molecules (Fig. 2(B)), which gave an excellent correlation coefficient (R) value of 0.85, Q2 value of 0.6 and Pearson-R value of 0.837. The validation indicates that the obtained QSAR model was good. Molecular docking studies were carried out for the all 100 dataset molecules which were used QSAR building. The obtained AADRR.10 model (Fig. 1) was used as a reference to design new and active inhibitors for EGFR by applying shape based screening analysis from in house library of twenty million molecules and 1436 conformers were obtained.

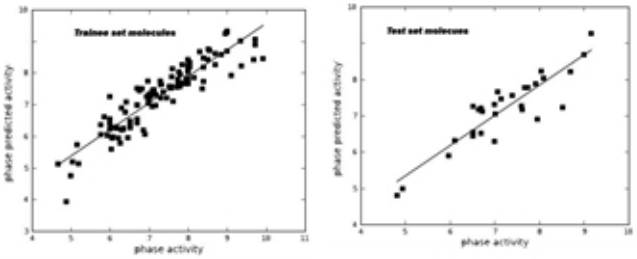

(A) (B)

Fig. 2: Scatter plots for the predicted and experimental pIC50 values of AADRR (A). Trainee set correlation (B). Test set correlation

TABLE:1D- QSAR PROPERTIES OF THE MODELAADRR.10

Factor	SD	R^2	F	P	RMSE	Q^2	Pearson-R
1	0.27	0.85	106.8	2.32e-13	0.29	0.629	0.837

4. RRD docking

Maestro v9.6 virtual screening workflow was used and sequential docking modes which were penalize the lesser steric classes to higher steric classes from HTVS to SP, XP docking and ranked based on the Gscore. 1436 conformers were obtained in HTVS and applied to SP; top 10% molecules (143) obtained from SP and applied to XP. The top 10 compounds were re-docked using Glide XP docking method. The top ranked ten molecules were compared with the binding interactions and XPG scores of published 100 inhibitors. The docking interactions of EGFR-lead 1 were analyzed and lead1 showed the docking score of -12.534 kcal/mol and good binding energy of -124.708 kcal/mol (TABLE 2). The good binding affinity of lead 1 was due to hydrogen bonding, hydrophobic interactions, hydrophilic interactions, electrostatic interactions, π cation and steric interactions (Fig. 3(B)).Lead 1 was bound to EGFR with four hydrogen bonds in addition to hydrophobic and van der Waal (vdW) interactions (Fig.3B). The H-atom of hydroxyl group (OH) and H atom of ((N)–H) of lead 1 formed two hydrogen bonds with inhibitor binding site residue Asp 800 with the distance of 1.778 Å and1.688 Å. The nitryl group (4(N)) of lead 1 formed hydrogen bond with inhibitor binding site residue Met793 with a distance of 1.05 Å and H-atom of hydroxyl group (OH) of lead 1 formed hydrogen bond with inhibitor binding site residue Cys797 with a distance of 1.2 Å. The residues Leu718, Gly719, Val726, Ala743, Ile744, Lys745, Mey766, Leu777, Leu788, Ile789, Thr790, Gln791, Leu792, Met793, Gly796, Cys797, Leu799, Asp800, Arg803, Arg841, Leu844, Thr854, Asp855, Leu858 and Met1002were involved in good van der Waals interactions with lead1 (Fig. 3(B)). Pharmacokinetic properties of lead 1 were well within the acceptable range of a drug (TABLE 2).The best ranked EGFR-lead 1 docking complex and inhibitors were applied to QPLD

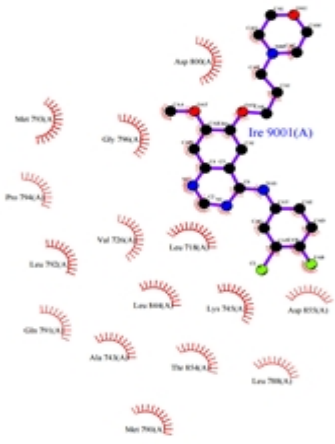

(A)

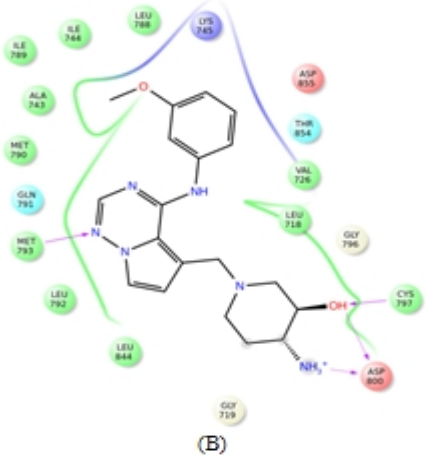

(B)

Fig.3. (A): 4I22- 2TBS interactions (B). EGFR-lead 1 docking interactions

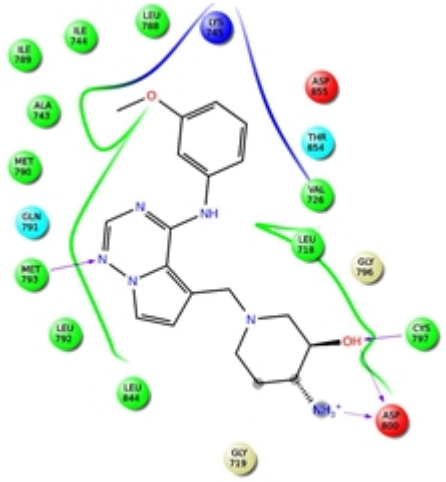

(A)

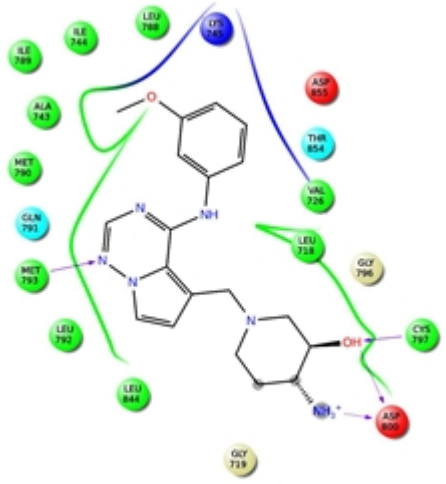

(B)

Fig.4: Llead 1 docking interactions with EGFR (A). QPLD (B). IFD

Lead 1 formed similar hydrogen bond interactions observed in RRD with XPG Score of -12.682 kcal/mol and binding energy of -130.012 kcal/mol (TABLE 1). IFD analysis also revealed the similar binding interactions in the EGFR-lead 1docked complex and showed more interactions and XPG scores than XP and QPLD (XPG Score = -14.126 kcal/mol; ΔG value = -139.012 kcal/mol) (TABLE 2 and Fig. 3). In the present study lead 1 was showing better docking scores and binding energy scores than the existing inhibitors in three modes of docking such as XP, QPLD and IFD (Fig.3(B) & Fig.4 (A) & (B)). Lead 1showed good binding energy, betterbinding orientations, having more interactions with good pharmacological properties (TABLE 3.) and also good drug-like properties than existing inhibitors.

Table: 2Docking scores and δg bind energy of lead 1 and inhibitors which were in clinical trails

Leads	XP Gscore (kcal/mol)	ΔG (kcal/mol)	QPLD Gscore (kcal/mol)	ΔG (kcal/mol)	IFD Gscore (kcal/mol)	ΔG (kcal/mol)
Lead1	-12.53	-124.7	-12.68	-139.0	-14.12	-139.01
Lapatinib	-11.47	-93.7	-11.22	-96.08	-12.47	-93.49
Gefitinib	-10.09	-98.0	-9.95	-98.41	-10.36	-94.99
Erlotinib	-9.88	-102.1	-6.62	-82.64	-11.28	-82.16
Afatinib	-9.04	-93.2	-9.98	-93.89	-12.86	-94.12

Table: 3.Admet properties of lead1

S.No	Pharmacokinetic properties	Lead 1
1	QPPMDCK	13.252
2	QPPCaco	29.132
3	QPlogPo/w	1.02
4	QPlogS	-1.644
5	QPlogPC16	12.895
6	Percent Human Oral Absorption	0
8	H-bond donors	4
9	H-bond acceptors	8.4
10	Molecular weight	368.438
11	QPlogHERG	-2.037
12	Rule of Five	0
13	Rule Of Three	1
14	QPpolrz	38.616
15	QPlogPoct	23.191
16	QPlogPw	16.79
17	CIQPlogS	-2.118
18	QPlogBB	-0.469
19	QPlogKp	-6.565
20	QPlogKhsa	-0.185
21	SASA	657.968
22	FOSA	239.048
23	FISA	139.758
24	WPSA	37.61
25	PISA	279.161
26	Volume	1164.384

Foot note:

	(Range 95% of Drugs)
MW = Molecular Weight	(130.0 / 725.0)
SASA =Total solvent accessible surface area	(300.0 /1000.0)
FOSA =Hydrophobic solvent accessible surface area	(0.0/750.0)
FISA =Hydrophilic solvent accessible surface area	(7.0/330.0)
PISA =Carbon Pi solvent accessible surface area	(0.0/450.0)
WPSA=Weakly Polar solvent accessible surface area	(0.0/175.0)
Volume=Molecular Volume (A^3)	(500.0 /2000.0)
Donor= Donor - Hydrogen Bonds	(0.0 /6.0)
Accpt HB= Acceptor - Hydrogen Bonds	(2.0/20.0)
LogP o/w = log P for octavo/water	(-2.0 /6.5)
Logs = log S for aqueous solubility	(-6.5 / 0.5)
CIlogS = log S - conformation independent	(-6.5 / 0.5)
LogBB = log BB for brain/blood	(-3.0 /1.2)
Log KP = log KP for skin permeability	(KP in cm/hr)
Log Khsa = log K hsa Serum Protein Binding	(-2.5 / 1.5)
Lipinski Rule of 5 Violations	(maximum is 4)
Jorgensen Rule of 3 Violations	(maximum is 3)

1. Molecular dynamics simulations

Simulation protocol provided exact binding orientations of the docking complex with system embedded with water molecules, temperature and pressure. After simulations, the docked complex of the EGFR-lead 1 energy was relatively stable throughout the 50 ns simulations period. Stability of the docked complex was compared with the co-crystal 4I22-2TB docking complex. During 50 ns simulations period, EGFR-lead 1docked complex showed stability in 10486 trajectories. In EGFR-lead 1docked complex RMSD of EGFR C-α showed 0.8 Å – 3 Å and lead1 was 0.6 Å – 2.4 Å (Fig. 4(A)). In 4I22-2TB docked complex, RMSD of EGFR C-α ranged from 1.6 - 3 Å.6 Å and lead1 ranged 0.8 – 3.6 Å (Fig .4(B)). Whereas RMSF of EGFR was ranged from 2 Å – 4 Å and lead 1 showed 0.6 Å - 0.8 Å in EGFR-lead 1docked complex (Fig. 5A & 6A). In case of 4I22-2TB docked complex, RMSF of EGFR was ranged from 0.5 Å – 4 Å and lead 1 showed 0.5 Å - 2 Å respectively(Fig. 5(B(& 6(B)) [37,38]. Lead 1 formed similar hydrogen bond interactions as observed in RRD, QPLD and IFD (Fig. 3(B), Fig. 4(A) & (B)). The small range of RMSDs and RMSFs reflected slight structural rearrangement in the docking complex during simulation time. The consistency of EGFR-lead1 docking complex was disclosed by the potential energy plot driven from the 50 ns simulations run in the solvated model system (Fig. 7(B)). The potential energy plot driven for EGFR-lead1 docking complex showed least energy than EGFR-2TB docking complex (Fig. 7(A)) and found to be stable throughout the simulations run. The RMSD, RMSF and energy plot of the EGFR- lead1 was stable than the 4I22- 2TB complex throughout the 50 ns simulations run.

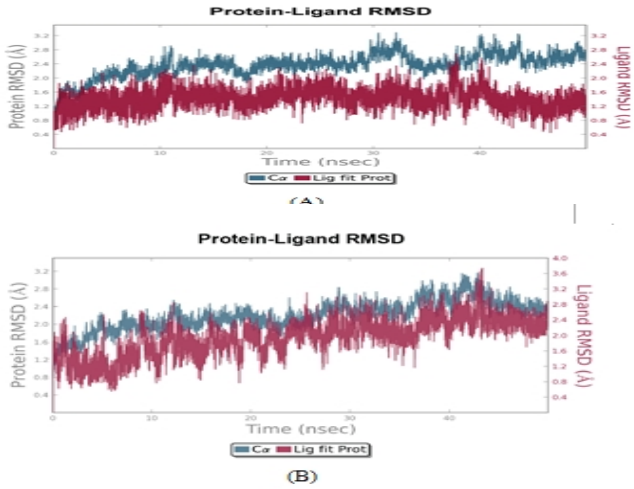

Fig.4: RMSD plots of EGFR protein with (A). Lead1 (B). Co-crystal ligand 2TB

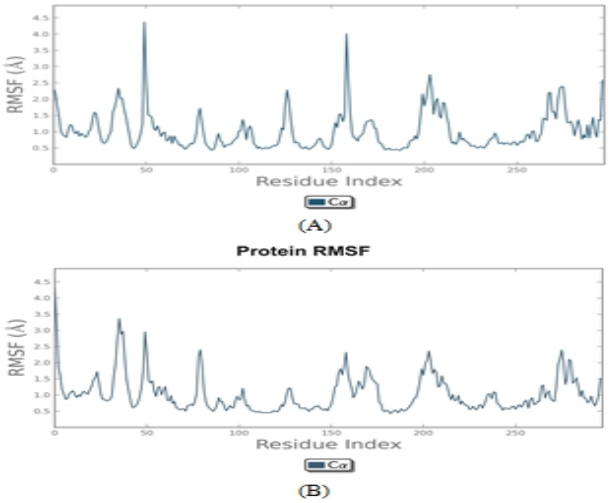

Fig.5: RMSF plots of EGFR c-α with (A). Lead1 (B). Co-crystal ligand 2TB

Lead 1 formed five hydrogen bonds interactions with inhibitor binding site residues of EGFR such as Met793 (2) Cys797, Asp800 (2) and four hydrophobic interactions were observed with inhibitor binding site residues Leu718, Ala743, Leu844, Lys745 (polar contact), and also formed charged interaction with important mutational residue Met790 (Fig. 8(A) & Fig. 9(A)). Ten water mediated interactions were observed with ligand binding site of residues of EGFRVal717, Leu718, Ser720, Lys745, Cys755, Met793, Cys797, Asp800, Thr854 and Asp855 (DFG residue)and it increased the binding affinity and entropy gain in the complex formation [39,40].

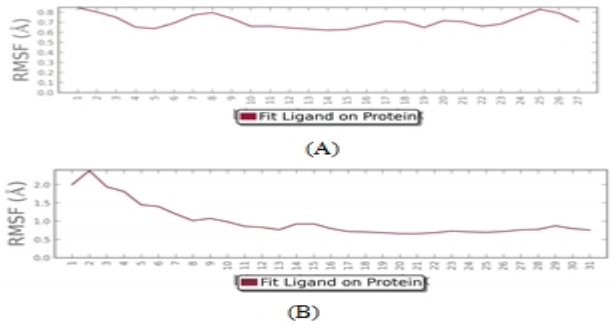

Fig.6: RMSF plots of (A). Lead1 (B). Co-crystal ligand 2TB with EGFR

C-crystal ligand 3BM formed one hydrogen bond interactions with inhibitor binding site residues of EGFR such as Met793 and hydrophobic interactions were observed with inhibitor binding site residues Leu718, Phe723, Val726, Ala743, Lys745, Met790, Leu792, Leu844 (Fig. 8(A) & 9(A)). The torsion angles were found to be stable within allowed range of fluctuations during all trajectories. Lead1 formed ten water mediated interactions were observed with ligand binding site of residues of EGFRVal717, Leu718, Ser720, Lys745, Cys755, Met793, Cys797, Asp800, Thr854 and Asp855 (DFG residue) and it increased the binding affinity and entropy gain in the complex formation (Fig. 8(A) & 9(A)). 3BM formed only four water mediated interactions with Leu718, Cys797, Asp800, and Arg841 (Fig. 8(B) & 9(B)). The torsion angles were found to be stable within allowed range of fluctuations during all trajectories in both the docking complexes (Fig. 10(A) & (B)). Over all analysis of RMSD, RMSF, potential energy, hydrogen bonding patterns, water bridges and torsion angles of EGFR-lead 1 docked complex in 10,416 trajectories revealed stability of docking complex in natural physiological environmental conditions and better when compare with the co-crystal structure .

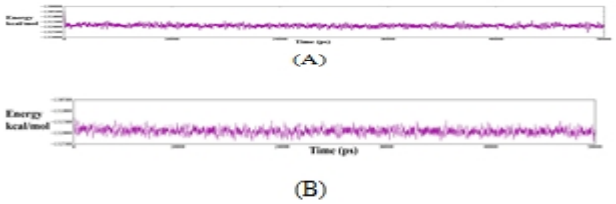

Fig.7: Energy plot of EGFR with (A). Lead1(B). Co-crystal ligand 2TB

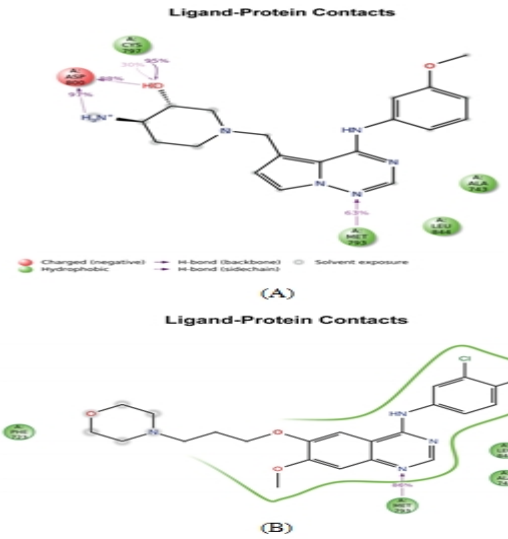

Fig.8: EGFR contacts with (A). Lead 1 (B). Co-crystal ligand 2TB

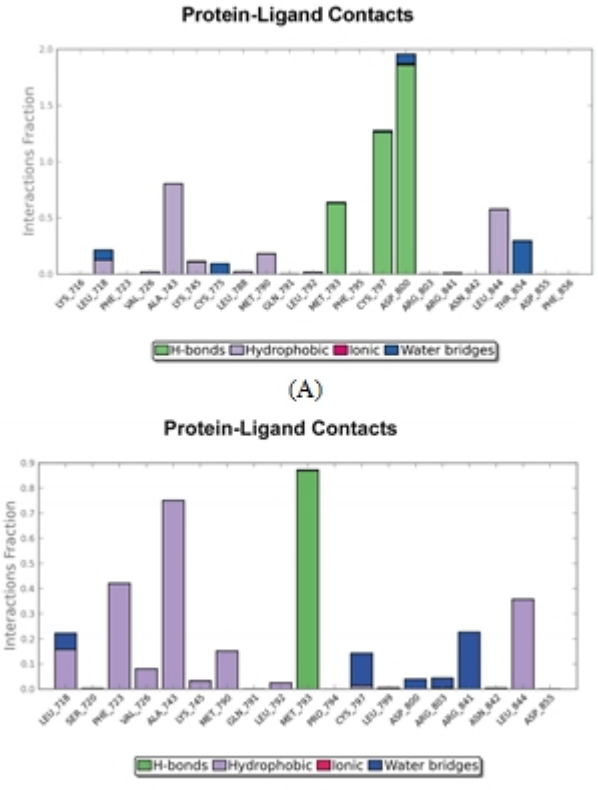

Fig.9: Interactions of EGFR with (A). Lead 1 (B). Co-crystal ligand2TB

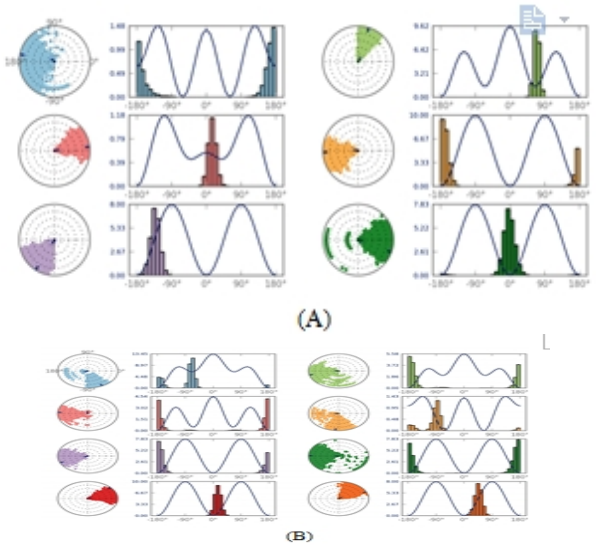

Fig.10: Torsion profile throughout the 50 ns molecular dynamics simulations period of (A). Lead1 (B). Co-crystal ligand 2TB

Lead 1 showed good binding energy in terms of XPG score and ΔG binding score in RRD, QPLD, IFD than the existing inhibitors and co-crystal ligand. It is having good pharmacokinetic properties and showed better interactions than Afatinib. Identified lead1 scaffold could be useful to develop novel inhibitor and in turn it helps to inhibit the over expression levels of EGFR in cancer condition.

Conclusion

Human EGFR is the most attractive target against the various cancers in drug development era. Ligand based pharmacophore modeling and 3D-QSAR analysis yielded five featured AADRR.10 pharmacophore model and showed correlation co-efficient with training set and test 0.84 and 0.81 respectively, suggesting the reliability of QSAR model. The model was screened against twenty million entries and obtained conformers were applied to RRD, QPLD and IFD and subsequent MM-GBSA analysis. Lead 1 showed better XPG score and free binding energy which revealed the potency interactions between protein and ligand. 50 ns MD simulations revealed acceptable range of RMSD, RMSF, and stability of the docking complex, total energy and better binding modes. Hydrogen bond interactions were observed inhibitor binding site residues of Met793, Cys797, Asp800, Leu718, Ala743, Leu844, Lys745 (polar contact), and charged interaction with important mutational residue Met790.Water mediated interactions were observed with inhibitor binding site residues of Val717, Leu718, Ser720, Lys745, Cys755, Met793, Cys797, Asp800, Thr854 and Asp855 (DFG loop).Obtained lead 1 possesses better XPG score in three modes of docking protocols, good binding interaction and binding energies with EGFR. Identified lead 1would act as the best inhibitor and also template for the development of novel inhibitors to interdict the adverse activity of EGFR in human cancers.

Acknowledgment

Authors are thankful to DBT, Ministry of Science and Technology, Govt. of India for providing support to SVIMS Bioinformatics through BIF program (No.BT/BI/25/001/2006) and SS is grateful to ICMR, New Delhi for providing SRF (No.BIC/11(09)/2013).

References

1. J. Schlessinger, “Common and distinct elements in cellular signaling via EGF and FGF receptors,” Science, vol. 306, pp.1506-1517, Nov 2004.
2. N. E. Hynes, G. MacDonald , “ErbB receptors and signaling pathways in cancer, ” Curr. Opin. Cell. Biol, vol. 21, pp. 177-184. Apr 2009.
3. Y. Yarden, M. X. Sliwkowski, “Untangling the ErbBsignalling network, ” Nat. Rev. Mol. Cell. Biol, vol.2, pp. 127-137, Feb 2001.
4. Jr. R. Roskoski, “The ErbB/HER receptor protein-tyrosine kinases and cancer,” Biochem. Biophys. Res. Commun, vol. 319, pp. 1-11, Jun 2004.
5. M. A. Lemmon, J. Schlessinger, “Cell signaling by receptor tyrosine kinases,” Cell, vol. 141, pp. 1117-1134, Jun 2010.
6. G. Lurje G, H. J. Lenz HJ, “EGFR signaling and drug discovery,” Oncology, vol. 77, pp. 400-410, April 2009.
7. C. H. Yun, K. E. Mengwasser, A.V. Toms, M. S. Woo, H. Greulich, K. K. Wong, M. Meyerson, M. J. Eck, “The T790M mutation in EGFR kinase causes drug resistance by increasing the affinity for ATP, “ Proc. Natl. Acad. Sci. U S A, vol. 105, pp. 2070–2075, December 2008.
8. H. Zhang, A. Berezov, Q. Wang, G. Zhang, J. Drebin, R. Murali, M.I .Greene, ErbB receptors: from oncogenes to targeted cancer therapies,’ J. Clin. Invest, vol. 117, pp. 2051-2058, Aug 2007.
9. W. Pao, J. Chmielecki, “Rational, biologically based treatment of EGFR-mutant non-small-cell lung cancer,” Nat. Rev. Cancer, vol. 10, pp. 760-774, Nov 2010.
10. M. A. Olayioye, R. M. Neve, H. A. Lane, N. E. Hynes, “The ErbB signaling network: receptor heterodimerization in development and cancer, “ EMBO. J, vol. 19, pp. 3159-3167, Jul 2000.
11. W. Zhou, D. Ercan, L. Chen, C. H. Yun, D. Li, M. Capelletti, A. B. Cortot, L.Chirieac, R. E. Iacob,R. Padera, J. R. Engen, K.K. Wong, M. J. Eck, N.S. Gray, P.A. Jänne, “ Novel mutant-selective EGFR kinase inhibitors against EGFR T790M,” Nature,vol. 462, pp. 1070-104, December 2009.

12. F. Bai, H. Liu, L. Tong, W. Zhou, L. Liu, Z. Zhao, X. Liu, H. Jiang, X. Wang, H. Xie, H. Li, "Discovery of novel selective inhibitors for EGFR-T790M/L858R," Bioorg. Med. Chem. Lett, vol. 22, pp. 1365-1370, Feburary 2012.
13. S. Li, C. Guo, X. Sun, Y. Li , H. Zhao, D. Zhan, M. Lan, Y. Tang, "Synthesis and biological evaluation of quinazoline and quinoline bearing 2,2,6,6-tetramethylpiperidine-N-oxyl as potential epidermal growth factor receptor(EGFR) tyrosine kinase inhibitors and EPR bio-probe agents," Eur. J. Med. Chem, vol. 49, pp. 271-278, March 2012.
14. G. J. Riely, "Second-generation epidermal growth factor receptor tyrosine kinase inhibitors in non-small cell lung cancer," J. Thorac. Oncol, vol. 3, pp. :S146-S149, June 2008.
15. C. M. Rocha-Lima, H. P. Soares, L.E.Raez, R. Singal R, "EGFR targeting of solid tumors,". Cancer. Control, vol. 14, pp. 295-304, July 2007.
16. F. Gazdar, "Activating and Resistance Mutations of EGFR in Non-Small-Cell Lung Cancer: Role in Clinical Response to EGFR Tyrosine Kinase Inhibitors," Oncogene, vol. 28, S24–S31, August 2009.
17. S. Kobayashi, H. Ji, Y. Yuza, M. Meyerson, K. K. Wong, D. G. Tenen, B. Halmos, "An alternative inhibitor overcomes resistance caused by a mutation of the epidermal growth factor receptor," Cancer Res, vol. 65, pp. 7096-101, August 2005.
18. Wissner, T. S. Mansour, "The development of HKI-272 and related compounds for the treatment of cancer," Arch. Pharm. (Weinheim), vol. 341, pp. 465-477, August 2008.
19. Li D, Ambrogio L, Shimamura T, et al. BIBW2992, an irreversible EGFR/HER2 inhibitor highly effective in preclinical lung cancer models. Oncogene. 2008;27(34):4702–4711.
20. J. A. Engelman, K. Zejnullahu, C. M. Gale, E. Lifshits, A. J. Gonzales, T. Shimamura, F. Zhao, P. W. Vincent, G. N. Naumov, J.E. Bradner, I. W. Althaus, L.Gandhi,G. I.Shapiro, J.M. Nelson, J.V. Heymach, M. Meyerson, K.K. Wong, P.A. Jänne, "PF00299804, an irreversible pan-ERBB inhibitor, is effective in lung cancer models with EGFR and ERBB2 mutations that are resistant to gefitinib," Cancer Res, vol. 67, pp. 11924-11932, December 2007.
21. R. C. Doebele, A.B. Oton, N. Peled, D.R.Camidge, P.A. Bunn Jr, "New strategies to overcome limitations of reversible EGFR tyrosine kinase inhibitor therapy in non-small cell lung cancer," Lung Cancer, vol. 69, pp. 1-12, July 2010.
22. Wissner, E. Overbeek, M.F.Reich, M.B.Floyd, B.D. Johnson, N. Mamuya, E.C. Rosfjord, C. Discafani, R. Davis, X. Shi, S.K. Rabindran, B.C.Gruber, F. Ye, W.A. Hallett, R. Nilakantan, R. Shen, Y.F. Wang, L.M. Greenberger, H.R.Tsou, "Synthesis and structure-activity relationships of 6,7-disubstituted 4-anilinoquinoline-3-carbonitriles. The design of an orally active, irreversible inhibitor of the tyrosine kinase activity of the epidermal growth factor receptor (EGFR) and the human epidermal growth factor receptor-2 (HER-2)," J. Med. Chem, vol. 46, pp. 49-63.January 2003.
23. Joshi M, Rizvi SM, Belani CP. Afatinib for the treatment of metastatic non-small cell lung cancer. Cancer Manag Res. 2015 Feb 19;7:75-82.
24. T. Liu, Y. Lin, X. Wen, R. N. Jorissen, M. K. Gilson, "BindingDB: a web-accessible database of experimentally determined protein-ligand binding affinities," Nucleic Acids Res., vol. 35, pp. 198-201, January 2007.
1. C. Selvaraj, S. K. Tripathi, K. K. Reddy, S. K. Singh, "Tool development for Prediction of pIC50 values from the IC50 values - A pIC50 value calculator," Curr. Trend. Biotech. Pharm, vol. 5, pp. 1104-1109, April 2011.